



Incremental Hole Drilling Residual Stress Measurement in Thin Aluminum Alloy Plates Subjected to Laser Shock Peening

J.P. Nobre^{1,2} · C. Polese^{1,3} · S.N. van Staden^{1,3}

Received: 6 July 2019 / Accepted: 24 January 2020 / Published online: 7 February 2020
© Society for Experimental Mechanics 2020

Abstract

The American standard ASTM E837 presents a standard procedure to determine residual stresses in isotropic materials using the incremental hole drilling technique (IHD). The standard, however, presents limitations regarding its applicability, such as those related with the thin thickness of the samples. According to this standard, in depth non uniform residual stresses can only be determined, roughly, in plates where the thickness is greater than the mean diameter of the strain gage rosette used. This limitation excludes important experimental cases and, therefore, deserves to be investigated. In this work this limitation is numerically and experimentally investigated in detail, considering the case of residual stresses induced by laser shock peening (LSP) in aluminum alloy 7075-T651 plates. The obtained results using the incremental hole drilling technique (IHD), based on the integral method, are benchmarked against the results of several diffraction techniques, used as reference, and a procedure to correct the experimentally determined strain-depth relaxation curves, to accurately still apply the ASTM E837 standard procedure is discussed and validated.

Keywords Residual stress · Hole drilling method · Thin plates, laser shock peening · X-ray diffraction · Neutron diffraction · Energy dispersive synchrotron X-ray diffraction

Introduction

The incremental hole drilling technique (IHD) is a well-established technique for measuring residual stresses induced by mechanical surface treatments [1, 2]. The laser shock peening treatment (LSP), imparting a deeper layer with beneficial residual compressive stress and decreasing surface roughness in comparison with conventional shot peening [3], improving fatigue and corrosion resistance, retarding or

even arresting fatigue crack growth [4], has received particular attention of the aeronautical and aerospace industries in recent years [5]. As it happens with other mechanical surface treatment techniques, such as, e.g., shot peening [3] or ball-burnishing [6], as a way for improving the LSP parameters, particularly in thin parts [7, 8], and to predict the surface integrity of the treated parts by numerical simulation, the IHD technique has been extensively used to determine the induced LSP residual stresses [9]. It should be noted that other residual stress measurement methods, such as the more recent contour method [10], which also enables mapping 2D residual stresses based on analytical solutions [11] or 3D residual stresses [12], through the whole section of the samples, can also be used for measuring residual stresses induced by LSP.

The ASTM E837 standard [1] describes a standard method to determining in-depth non-uniform residual stresses by the incremental hole-drilling technique in workpieces thicker than the diameter of the gauge circle (D to $1.2D$), depending on the standard strain-gauge rosette used, type A or B and type C, respectively [1]. For thinner workpieces ($0.2D$ (type A or B) to $0.24D$ (type C)), the standard only describes the method for determining in-depth uniform residual stresses using a through hole. Thus, the standard cannot be applied to

✉ J. P. Nobre
joao.nobre@wits.ac.za

C. Polese
claudia.polese@wits.ac.za

¹ School of Mechanical, Industrial and Aeronautical Engineering, University of the Witwatersrand, Johannesburg, South Africa

² CFisUC - The Centre for Physics of the University of Coimbra, University of Coimbra, Coimbra, Portugal

³ DSI-NRF Centre of Excellence in Strong Materials, hosted by the University of the Witwatersrand, Johannesburg, South Africa

determine in-depth uniform or non-uniform residual stresses in “thin” samples, i.e., for samples with thicknesses ranging from $0.2D_0$ to D_0 . To mitigate this problem, some authors have proposed that an epoxy backing could be adhesively applied to the back of thin specimens to artificially increase their thickness [13, 14], or simply apply the standard method without correction [8, 15]. However, some authors have proposed correction procedures [16] to still apply the ASTM E837 standard procedure for “thick” samples in these cases [1]. According to Sobolevski [17] the thickness limits presented by the standard [1] are conservative, proposing a limit of $1.66D_0$, where D_0 is the hole diameter, which is substantially lower than the limit preconized by the ASTM standard. Held et al. [16] pointed out that, for a 2.5 mm thick plate and 1.8 mm hole diameter, the maximum deviation falls within 5%, considering an in-depth uniform equibiaxial stress. This thickness corresponds to half of the limit preconized by the standard [1] (5.13 mm for type A and B rosettes). With decreasing thickness, the evaluated stress increases and the stress distribution is not constant in depth anymore [16]. Near the surface, for depths up to 0.7 mm, the stress is almost constant, but strongly overestimated due to the lower effective local stiffness [16]. For larger drilling depths the stress significantly decreases, which should be due to the changes in the effective local stiffness [16]. According to their findings, Held et al. [16] proposed a correction approach to still use the ASTM standard “thick” calculation procedure [1] in thin samples. Their approach is based on the application of a correction function for the measured strain relaxations, prior to the stress calculation using the standard procedure. In short, in “thin” samples falling out of the standard limits, the measured strain relaxation should be first corrected based on a correction function $L_{geometry}(t_n, z)$, using [16]:

$$\varepsilon_{corrected}(z) = L_{geometry}(t_n, z) \cdot \varepsilon_{thin\ component}(t_n, z) \quad (1)$$

Where:

$$L_{geometry}(t_n, z) = \frac{\varepsilon_{standard}(z)}{\varepsilon_{thin\ component}(t_n, z)} \quad (2)$$

$\varepsilon_{standard}(z)$ is the strain relaxation of a corresponding “thick” standard component, within the application limits, through the hole depth (z) and $\varepsilon_{thin\ component}(t_n, z)$, the strain relaxation field determined in the actual “thin” component, as a function of the hole depth (z), for a specific normalized component’s thickness $t_n = t/D_0$, where t is the sample thickness and D_0 the hole diameter. Both strains are determined by FE-analysis considering the same D_0 , rosette geometry (ASTM type B rosette), material (E, ν) and stress state. The difficulty of this approach relies with the difficulty to determine such correction function $L_{geometry}(t_n, z)$ [16]. However, the effort is lower than that necessary to recalculate the necessary calibration coefficients for the integral method, the IHD residual stress calculation procedure,

widely accepted, to relate the relieved strains and the existing residual stress [1, 18, 19]. In addition, when several components with different thickness (“or with further geometry features that deviate from the ‘standard’” [16]) have to be analyzed, the effort can significantly be reduced using a simple linear interpolation of $L_{geometry}$ values, since the error of an interpolation within a normalized thickness increment $\Delta t_n = 0.25$ is less than 1%. An improved method can be based on the application of artificial neural networks [16]. If effective, this procedure is very convenient since it avoids specific numerical simulation, case by case, when the component’s thickness is lower than the limit announced by the standard, as performed in [20]. For it, as shown by Magnier et al. [20], care must be taken when constraining the model during the finite element analysis for the determination of the necessary calibration constants for the integral method. Moreover, the solution for this problem seems to be worse when the residual stress approaches the material’s yield stress and there could be plasticity effects [1, 21, 22].

The feasibility of the correction procedure described above for the case of laser shock peening stresses will be analyzed in detail in this work. Residual stresses in aluminum AA7075 alloy plates, with different thicknesses and subjected to laser shock peening (LSP), using the same LSP parameters, are determined by IHD using the integral method [18, 23]. The samples with dimensions outside of the standard are tested both with and without an epoxy backing support and the residual stresses measured are compared to those measured in samples falling within the standard. The results are benchmarked against the results obtained by diffraction techniques, used as reference, such as neutron diffraction (ND), energy dispersive X-ray diffraction (EDXRD) and laboratory X-ray diffraction (XRD). In addition, two finite element models were developed. Firstly, a numerical simulation by the finite element method (FEM) is carried out to determine the expected strain relaxation errors due to the thin thickness of the samples, falling outside the limits preconized by the ASTM standard. Secondly, the necessary calibration coefficients for the integral method, considering the actual thickness of the samples, are determined by FEM. This way, the feasibility of the above mentioned correction procedure, to still use the ASTM standard to accurately determine non uniform residual stresses in thin samples, is discussed and validated. The validation is achieved by comparing the IHD corrected results with the results obtained by the cited reference techniques and with the IHD results, based on the integral method using the necessary calibration coefficients for the actual thickness of the samples.

Materials and Methods

Samples of aluminum alloy 7075-T651 were machined from a single 15 mm thick rolled plate. The samples were prepared



with 10 mm, 6 mm, 3 mm and 1.6 mm thicknesses using the procedure described in Fig. 1. 10 mm and 6 mm plate thicknesses fall inside the limits preconized by the ASTM E837 standard, while 3 mm and 1.6 mm plate thicknesses, which are representative of conventional thicknesses used in aeronautical airframe structures, fall outside those limits. The mechanical properties and the chemical composition of the material are shown in Table 1.

The laser shock peening treatment (LSP) was performed at the National Laser Centre (NLC) of the Council for Scientific and Industrial Research (CSIR) in Pretoria, South Africa, using a Quanta-Ray Pro Spectra Physics (QRPSP) Nd:YAG laser. The QRPSP laser specifications and the LSP parameters are shown in Table 2. A spot sequence strategy is achieved using an X-Y raster pattern with equidistant spot placement in the horizontal and vertical directions. A 1.5 mm spot diameter was used to attain a power intensity of 3 GW/cm², with a spot density of 5 spots/mm² (~70% spot overlap). Figure 2 shows the final dimensions of each sample (Fig. 2a)), the laser scanning strategy for the LSP treatment performed (raster pattern) (Fig. 2b)), with the parameters referred in Table 2, and the measurement references for the determination of the residual stresses, using the incremental hole drilling (IHD), neutron diffraction (ND), energy dispersive synchrotron X-ray diffraction (EDXRD) and laboratory X-ray diffraction (XRD) (Fig. 2c)).

The incremental hole drilling was carried out using a SINT MTS3000-Reston equipment, standard ASTM E837 type A stain gage rosettes (1/16 in. nominal) and tungsten carbide inverted cone end mills, with typical 1.6 mm average diameter, for a final typical 1.8 mm hole diameter. Small drilling depth increments of 0.02 mm were used up to 1.2 mm total hole depth. The obtained strain-depth relaxation curves were smoothed using splines and the calculations were then performed considering minimum depth increments of 0.05 mm, as recommended by the ASTM E837 standard [1]. The residual stresses, based on the integral method coupled with the Tikhonov regularization [1], were determined using an own made software written in Python [18].

Neutron diffraction (ND) was performed to investigate the residual stresses through the depth of the samples. Neutrons are capable of penetrating deeper into aluminum, so it was possible with this technique to measure the residual stresses through the entire depth of the samples, despite its poor spatial

resolution. This technique could be used to validate the IHD results as well as complement them. However, the results near the surface would require validation by techniques better suited to near-surface measurements, such as laboratory X-ray diffraction. ND was used in this study to determine residual stresses in the 6 mm and 1.6 mm thick Al alloy samples, before and after LSP, as per Table 2. ND measurements were performed on the same sample (in the centre of the sample and on a peened patch, respectively), using the facilities of the Materials Probe for Internal Strain Investigations (MPISI) at the Safari-1 nuclear research reactor at Necsa - the South African Nuclear Energy Corporation Limited. The beam was monochromatic with a wavelength of 1.67 Å. A gauge volume of 0.3 mm × 0.3 mm × 10 mm was used and the d-spacing of the {311} lattice plane was measured around a 2θ angle of 85.5°. The 10 mm length was aligned parallel to the surface and 0.44 mm length was aligned through the depth. This shape and orientation was chosen because LSP residual stresses requires as small a gauge volume as possible to measure the high gradient residual stresses near the surface, while ND technique requires as large a gauge volume as possible to improve neutron counting statistics.

For validation purposes energy dispersive synchrotron X-ray (EDXRD) measurements were performed at the 6-BM-A beamline at the Advanced Photon Source (APS) at Argonne National Laboratories, USA. This synchrotron is extremely powerful and, therefore, with a fairly small beam, determination of residual stresses through the entire depth is also possible, moreover, with better resolution than what is possible with neutron diffraction. However, this method also requires additional near-surface validation by more suitable techniques, such as laboratory X-ray diffraction. For comparison purposes, the tests were performed in the same LSP samples analyzed by ND. The beamline is fitted with two detectors at fixed 2θ angles of −5.0° and 4.8°, for the vertical and horizontal, respectively. The beam was polychromatic with an energy range of 0–285 keV, which is sufficient to measure the first five peaks of FCC aluminum. The slits on the beam and both detectors were all set to 0.1 mm × 0.1 mm. Although it was possible to make them smaller, a larger dimension was chosen to improve X-ray count statistics. The beam slit sizes and detector direction angles created an elongated gauge volume, with a long side of 2.6 mm.

Fig. 1 Samples preparation

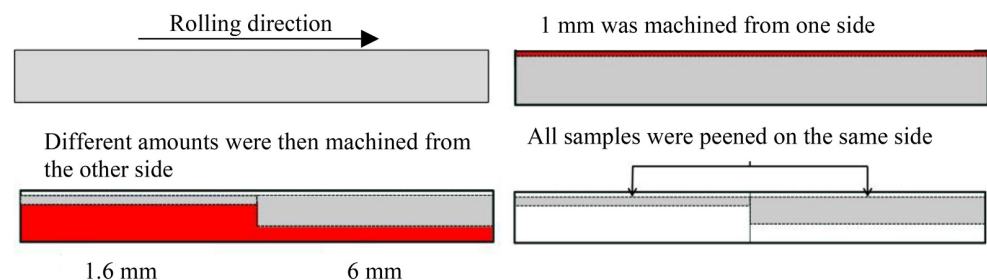


Table 1 Mechanical properties and chemical composition of the aluminum alloy 7075-T651 [24, 25]

Bulk Young's Modulus [GPa] ¹	Bulk Poisson's Ratio ¹	Tensile Yield Strength [MPa]	Chemical Composition Wt. [%]								
			Al ²	Cr ²	Cu ²	Fe ³	Mg ²	Mn ³	Si ³	Ti ³	Zn ²
71.7	0.33	503	89.3	0.23	1.6	0.5	2.5	0.3	0.4	0.2	5.6

¹ 69 GPa and 0.35 for the Young's modulus and Poisson's ratio for the {311} lattice plane, respectively

² Average value

³ Maximum value

In addition, laboratory X-ray diffraction (XRD) was used to obtain reference values at surface of the same LSP samples, since the minimum evaluation depth for the ND and EDXRD techniques was set to 0.1 mm and 0.06 mm, respectively. XRD was performed using the Bruker D8 Discover equipment at Necsa, South Africa. The $\sin^2\psi$ method [26] was used to determine the residual stresses by XRD. Lattice deformations related to the {311} planes were determined for 16 ψ angles between -45° and $+45^\circ$ using Cu-K α radiation. Measurements were taken at a total of 6 ϕ angles to obtain the planar stress-tensor. The residual stresses were calculated for the plain stress conditions using X-ray elastic constants (XEC) of $\frac{1}{2}s_2 = 1.95652174 \times 10^{-6} \text{ MPa}^{-1}$ and $s_1 = -5.07246377 \times 10^{-6} \text{ MPa}^{-1}$.

Finally, a finite element analysis was performed, using ANSYS Mechanical APDL code, to study the effect of strain relaxation in plates of different thicknesses subjected to the same equibiaxial stress state that, despite the slight differences observed in the experimental residual stress results measured in perpendicular directions, is close to the experimentally observed in this work and is of easy implementation using a 2D axisymmetric model. Since the plates are large enough to avoid border effects (except due to the thickness), the material is isotropic, the stress concentration is a local phenomenon and the stresses measured in different directions are similar, a 2D axisymmetric model can be used to determine the strain relaxation measured near the hole (around 2 mm hole diameter). In addition, IHD measurements were performed in the center of LSP area, which is also centered in the plate – see Fig. 2. A second finite element model (FEM) was developed to determine the necessary calibration coefficients for the implementation of the integral method, as per the ASTM E837 standard, to the thinnest plates experimentally analyzed. In both cases the 2D axisymmetric finite element model (FEM) was developed using 4-node axisymmetric solid elements

SOLID272, enabling modelling axisymmetric solids with axisymmetric or nonaxisymmetric loading [27]. In the first model, strain-depth relaxation curves corresponding to the same equibiaxial stress state were determined for different plate thicknesses, considering the standard strain gauge rosettes used in the experiments (type A). The in depth stress profiles, corresponding to those experimentally determined, were generated using temperature gradients introduced into a full constrained model before hole simulation. The incremental hole drilling was then numerically simulated using the “birth and death” of elements of ANSYS code features [23]. All elements existing at each incremental depth (0.02 mm each) were first selected and then “killed”, before solving the model (mapped mesh) shown in Fig. 3. A constant incremental depth of 0.02 mm was used up to a total 1 mm hole depth, i.e., for a total of 50 incremental steps. In the second model, for the same rosettes, the necessary calibration coefficients for the integral method were determined using an equibiaxial stress state for constant a and a pure shear stress state for constant b , to be used with the software developed in Python [18]. The determination of these calibration coefficients using 2D axisymmetric finite element model was first described by Schajer [19, 28]. The nodal strain values determined by FEM were integrated over the strain gage grid [29, 30] in both FE-analysis.

Results

LSP Residual Stresses by Diffraction

Figure 4 shows the residual stress results determined by neutron diffraction (ND) in 1.6 mm (Fig. 4a) and 6 mm (Fig. 4b) thick

Table 2 Laser specifications and laser shock peening (LSP) parameters used in this study

QRPS Laser Specifications						LSP Parameters		
Laser Type	Wavelength [nm]	Pulse Frequency [Hz]	Energy Range [J]	Spot Shape	Spot Size Range [mm]	Power Intensity [GW/cm ²]	Spot Diameter [mm]	Coverage [spots/mm ²]
Nd:YAG	1064	20	0.2–1	○	0.5–2.5	3	1.5	5



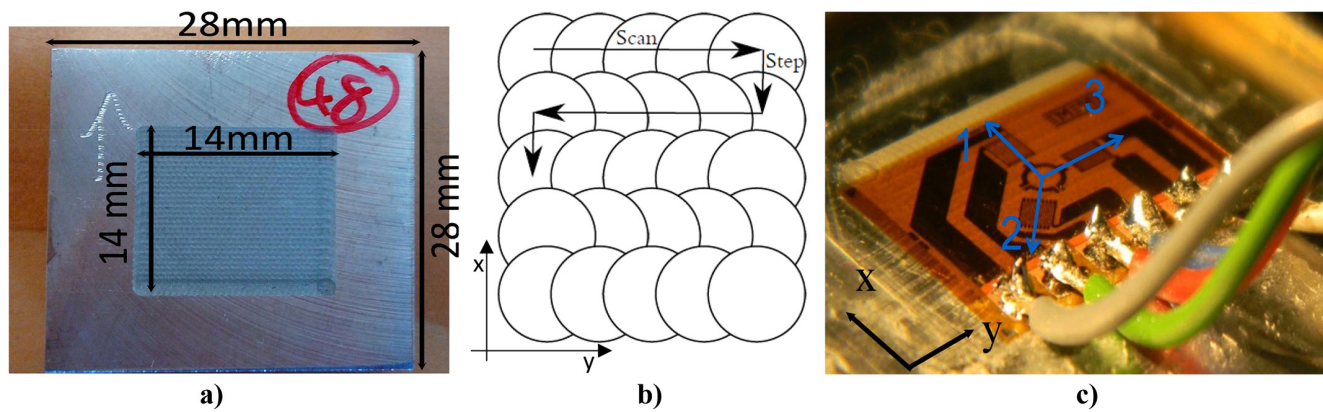


Fig. 2 a) Samples dimension, b) LSP scanning strategy and c) measurement references for the different residual stress techniques used (ND, EDXRD, XRD and IHD)

AA7075 alloy samples, before (as-machined) and after laser shock peening (LSP) using the parameters shown in Table 2. For validation purposes, Fig. 4 also presents a comparison with the residual stresses determined by energy dispersive synchrotron X-ray diffraction (EDXRD). It is clear that both measurement techniques present similar results through the thickness of the samples. Compressive residual stresses determined in the 1.6 mm thick samples are of a lower magnitude than those determined in the 6 mm thick samples. This is attributed to a spring back effect related with the fact that there is less elastic material responding to the plastic deformation induced by the LSP process, resulting in deformed samples with lower magnitude residual stresses. In addition, the fact that the area subjected to LSP is lower than the total area of the samples, together with the spring-back self-equilibrium effect, might explain the apparent lack of stress equilibrium shown in Fig. 4a – see also reference [8]. A study on the maximum out-of-plane deformation induced by LSP in the samples with different thicknesses was performed. The deformation increases with a decrease in thickness of the samples. While for 10 mm thickness the observed deformation was negligible, it attained 0.15 mm, 0.46 mm and 1.4 mm for samples with 6 mm, 3 mm and 1.6 mm thicknesses, respectively.

Finally, since the minimum evaluation depth for EDXRD and ND was 0.06 mm and 0.1 mm, respectively, both techniques are not suitable to determine the high stress gradients near the surface. For this reason, the results presented in Fig. 4 were complemented by laboratory X-ray diffraction (XRD) residual stress measurements. In the near surface layers, XRD results are the best reference for the results determined by IHD, as it will be seen in the following.

LSP Residual Stresses by Incremental Hole Drilling (IHD)

Figure 5a shows the residual stress (maximum principal stress) resulting from four tests performed in four 10 mm thick samples, subjected to the same LSP parameters - see Table 2. The IHD residual stress results present good repeatability, considering the tests were performed at different LSP spots. In Fig. 5b a comparison between the residual stress determined in the laser stepping direction (S_x) and in laser scanning direction (S_y) is made for 1.6 mm and 10 mm thick samples. The results show that the residual stresses in samples peened with a LSP raster pattern strategy induces residual stresses that are slightly different in the laser stepping direction, when

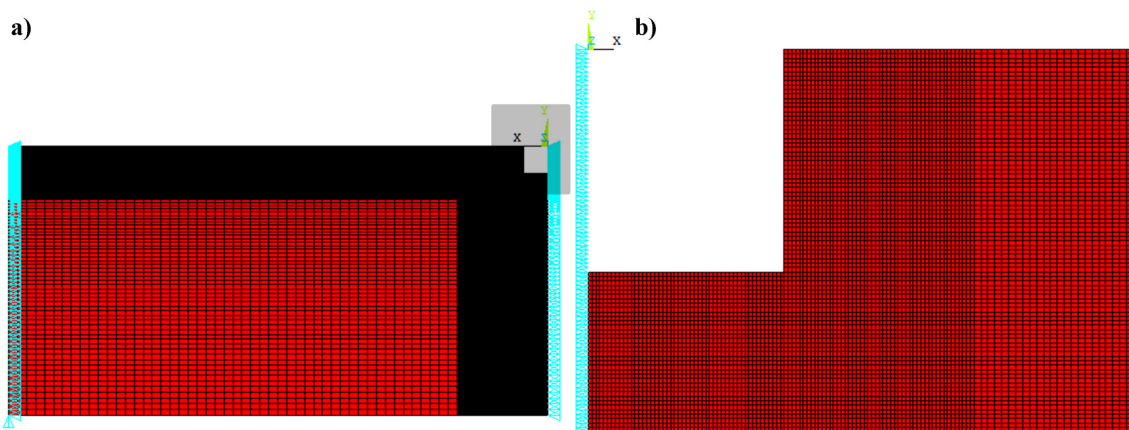


Fig. 3 FEM mesh for the 10 mm thick plate. a) Constraints used and b) amplification near the hole (with 1 mm depth) (grey area in Fig. 3a)

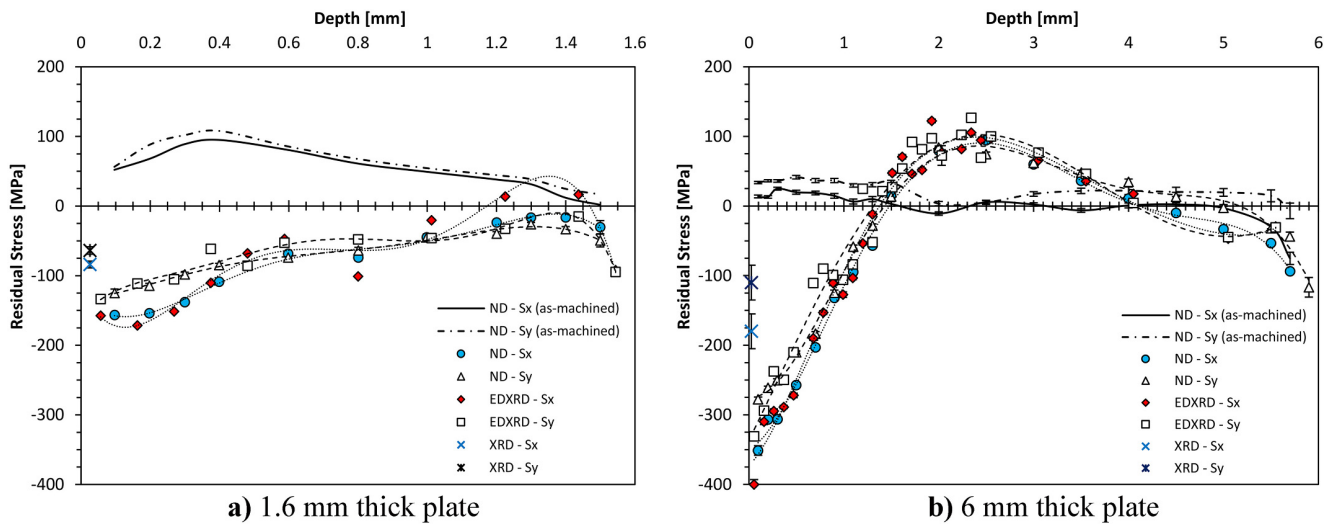


Fig. 4 Residual stresses determined by ND, EDXRD and XRD in the laser stepping direction (S_x) and in the laser scanning direction (S_y), before (as-machined - only ND) and after LSP in **a)** 1.6 mm and **b)** 6 mm thick plates. All lines are referred to curve fitting by polynomial interpolation

compared to the laser scanning direction, in particular for 1.6 mm thick plate. As observed in Fig. 5b, the magnitude of the induced compressive residual stress is systematically higher in the laser stepping direction than in the laser scanning direction, as also observed in Fig. 5. Correa et al. [31] also reported that samples peened using LSP raster pattern strategy usually presents differences in the residual stresses measured in perpendicular directions than those produced using a LSP random pattern strategy. In addition, the residual stresses present a lower magnitude in the thinner sample plates than in the thicker ones. The residual stress results determined by ND and EDXRD, shown in Fig. 4, also confirm these findings.

The averaged residual stresses determined by IHD in all samples, with different thicknesses, are presented in Fig. 6.

The residual stress values correspond to the minimum principal stress that, being compressive, presents the maximum magnitude. The error bars correspond to the sample standard deviation observed in at least three performed tests.

From the results presented in Fig. 6a it is clear that decreasing the sample thickness, the magnitude of the LSP residual stress decreases, as well as the depth affected by the LSP treatment, which was confirmed by the microhardness readings performed over the cross section of the samples. This finding is in line with the results determined by ND and EDXRD, as described in section 3.1. In Fig. 6b the results determined in LSP samples using an epoxy backing support, to mitigate the thin thickness of the sample plates, are compared with those determined without this strategy. As it can be

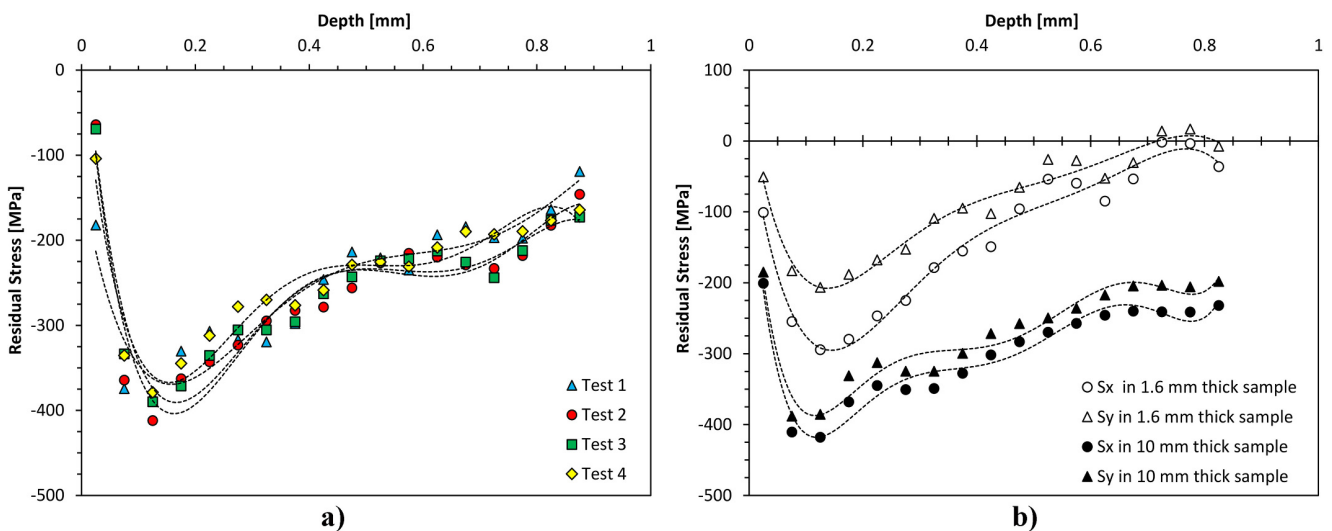


Fig. 5 **a)** Maximum principal residual stress determined in four 10 mm thick samples and **b)** Residual stresses in the laser stepping direction (S_x) and in the laser scanning direction (S_y) in 1.6 mm and 10 mm thick plates – LSP parameters according to Table 2. Dashed lines – curve fitting by polynomial interpolation



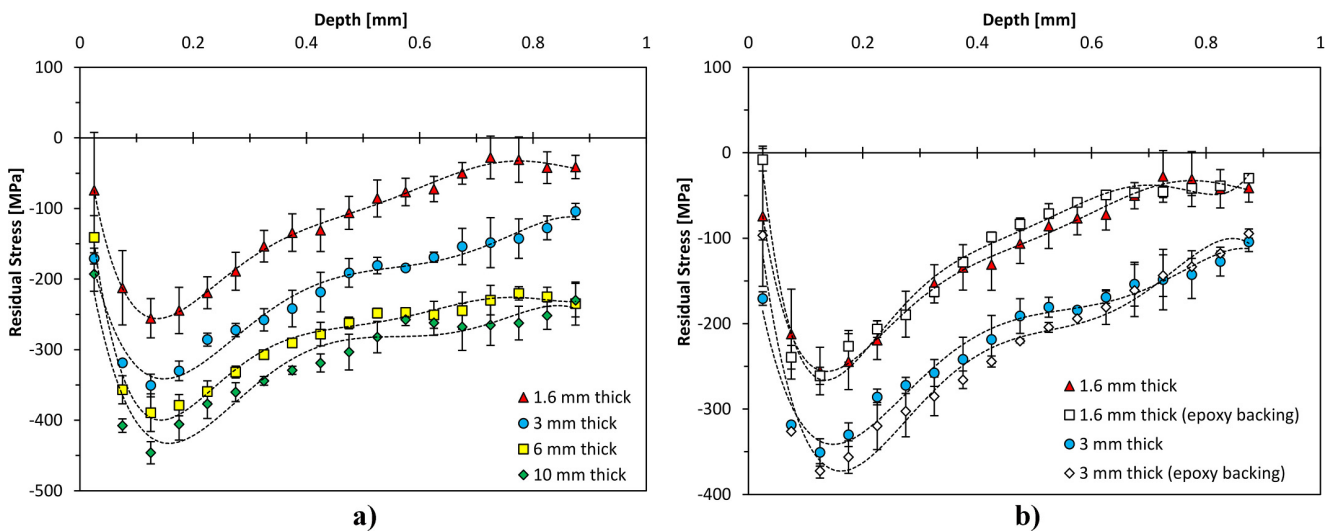


Fig. 6 a) Averaged minimum principal residual stress determined by IHD in LSP samples, in 1.6 mm, 3 mm, 6 mm and 10 mm thick samples and b) in 1.6 mm and 3 mm thick samples with and without epoxy backing strategy

observed, the use of this epoxy support does not significantly affect the residual stress measurements, since all results are within the measured uncertainty.

In Fig. 7 a comparison between the residual stress results determined by all residual stress measurement techniques, i.e., incremental hole drilling (IHD), laboratory X-ray diffraction (XRD), neutron diffraction (ND) and energy dispersive synchrotron X-ray diffraction (EDXRD), is shown for 6 mm and 1.6 mm thick samples, respectively. For a sake of clarity the comparison is only made for the residual stresses determined in the laser stepping direction (S_x), since the same trend is observed for the residual stresses in the laser scanning direction (S_y).

For 6 mm thick samples and deeper layers (> 0.06 mm depth), the residual stresses obtained by IHD agree well with those obtained by ND and EDXRD (Fig. 7a), despite the slight

overrating, lower than 50 MPa, observed on the IHD results at depths between 0.08 mm and 0.3 mm. Near the surface (< 0.06 mm depth), ND and EDXRD are not suitable to determine the high stress gradients. In these layers, XRD results are the best reference and the results determined by IHD agree well with those determined by XRD, considering the uncertainty always observed in the IHD residual stress results in the first depth increment (due to, e.g., zero at surface and roughness). The XRD was estimated to measure at a depth of 0.026 mm using the AbsorbDX software supplied by Bruker Corporation and the middle point for the first depth step of the IHD results is 0.025 mm and, therefore, the results of the two techniques can be directly compared. Note that, using a type A standard rosette, according to the ASTM E837 standard, the IHD evaluation is limited to a minimum plate thickness of 5.13 mm (D) [1]. The 6 mm plate thickness in this case fulfil

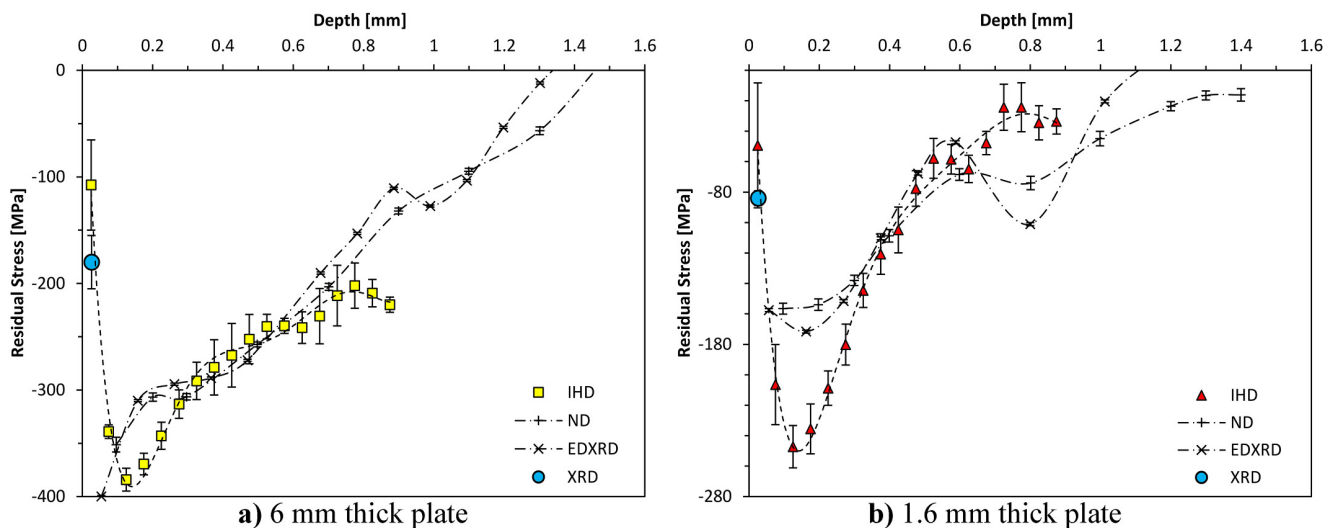


Fig. 7 Residual stress in the LSP step direction (S_x) determined by IHD, ND and EDXRD in a) 6 mm and b) 1.6 mm thick plates

this limit and no influence of a thin thickness is expected. However, for 1.6 mm thick samples, as shown in Fig. 7b, clear discrepancies between IHD and the other techniques (ND and EDXRD) are observed throughout the whole evaluation depth. IHD clearly overestimates the residual stress values underneath the surface, through the important region between 0.1 mm and 0.4 mm hole depth. An overrating around 100 MPa is observed between IHD and the other techniques. For deeper layers, the underestimation should be related with the changes in the effective local stiffness of the thin plates in the IHD results, as pointed out by Held et al. [16].

Discussion

To better understand the discrepancies observed between IHD and the other techniques for the case of the thinner samples, a finite element simulation (FEM) was performed. The cases under analysis are those related with the LSP samples with 1.6 mm and 3 mm thicknesses, which are falling out of the standard limits [1] ($< D = 5.13$ mm thickness). Considering an in-depth equibiaxial residual stress distribution, whose the profiles are shown in Fig. 6, strain-depth relaxation curves for the LSP samples were determined by FEM. For both cases, calculations were performed considering the real thickness of 1.6 mm and 3 mm, respectively, thus, enabling the determination of $\varepsilon_{\text{thin component}}(t,z)$ and also, using the same stress distribution, the strain relaxation values for a standard evaluation $\varepsilon_{\text{standard}}(t,z)$, i.e., considering that stress distribution is occurring in a plate thicker enough (10 mm), to fall within the standard limits [1] (see eqs. 1 and 2). Figure 8 shows the experimental IHD stress profiles considered, the stress distribution calculated by FEM, before the simulation of the first hole depth increment, and the stress determined by the integral

method using the FEM calculated strain-depth relaxation curves, after hole simulation.

The results obtained by the integral method, using as input the FEM simulated strain-depth relaxation curves, agree very well with the stress profiles used as input for the FEM model, which validates the FEM model used. The incremental hole drilling was numerically simulated using the “birth and death” of elements ANSYS code features [32], considering the in-depth stress profiles depicted in Fig. 8. The numerical simulation was performed considering plates with the actual thickness (1.6 mm and 3 mm, respectively) and plates thick enough (10 mm), to fall within the limits preconized by the ASTM standard. In Fig. 9 the von Mises stress field and the von Mises strain field around holes with 1 mm depth, for the hole diameter measured during the IHD experimental evaluation, are shown for the case of the “thick”, or standard, plate and for the actual plate with 1.6 mm thickness. All figures are represented with $\frac{1}{4}$ axisymmetric expansion and magnified with a scale factor of 100.

From Fig. 9 is possible to see (by the plot results in Fig. 9 c) and d), where the deformed shapes with undeformed edges are also shown) that the displacements are greater for the case of 1.6 mm plate thickness, compared to the case of a thick plate (10 mm) subjected to the same in-depth stress profile. The corresponding strain-depth relaxation curves calculated by FEM are shown in Fig. 10a, for this particular case (1.6 mm thick plate). In Fig. 10b the obtained results for the case of 3 mm plate thickness are also shown. Fig. 10 compares $\varepsilon_{\text{standard}}(z)$, which is the strain relaxation of a corresponding “thick” standard component, i.e. within the ASTM application limits, through the hole depth (z) and $\varepsilon_{\text{thin component}}(z)$, the strain relaxation field determined in the actual “thin” component, as a function of the hole depth (z), for the same in depth stress profile shown in Fig. 8. Therefore, the differences

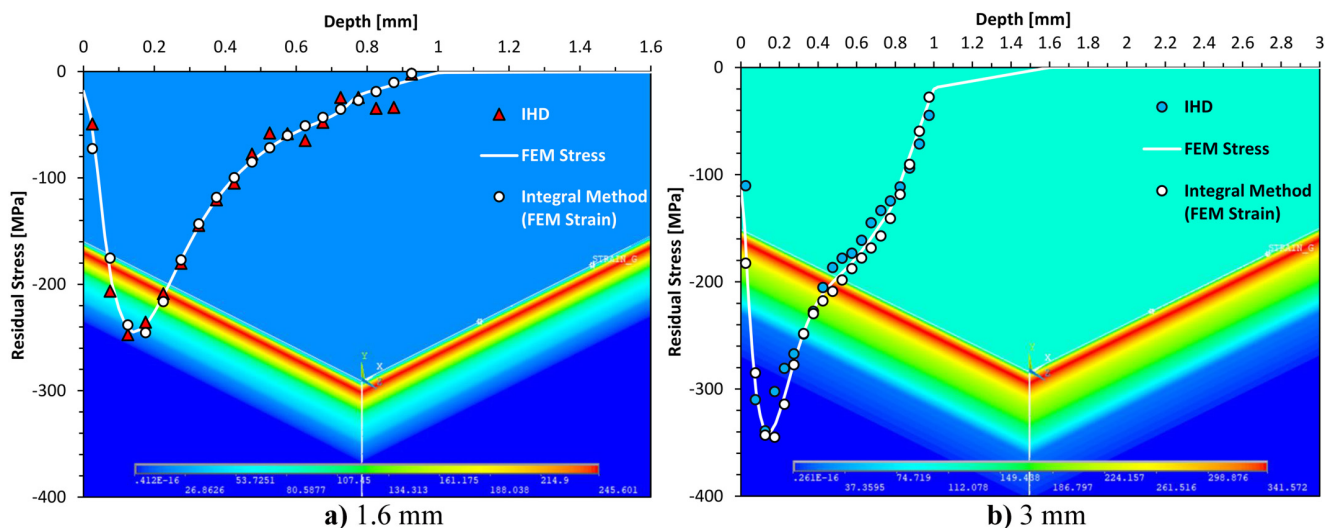


Fig. 8 Residual stress distribution determined during the experimental IHD tests, stress distribution determined by FEM before the hole simulation and stress distribution determined by the integral method based on the FEM strain-depth data after hole simulation for **a)** 1.6 mm and **b)** 3 mm thick plates

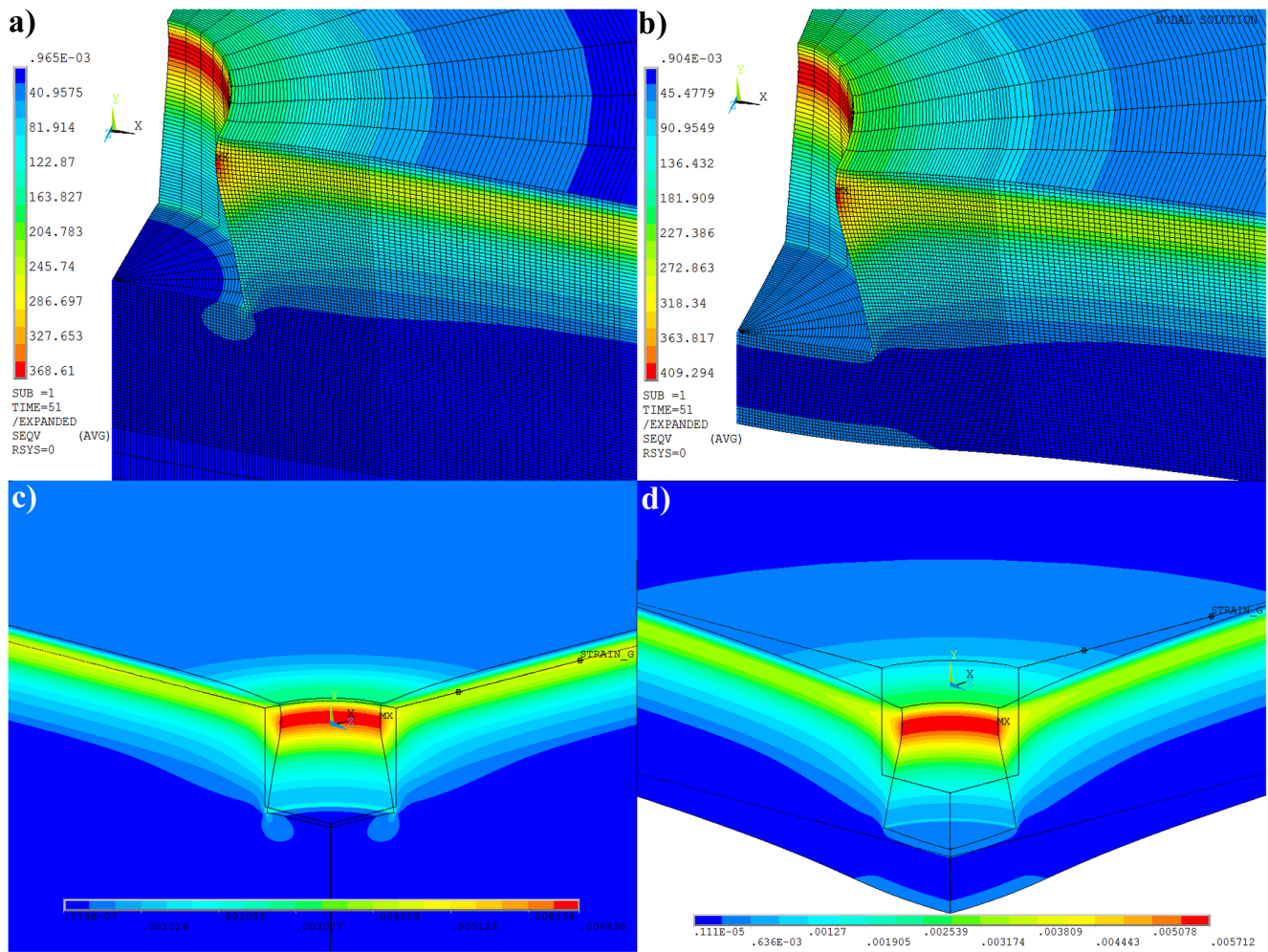


Fig. 9 a) and b) von Mises stress field and c) and d) von Mises strain field around a 1 mm hole depth, corresponding to the stress distribution determined in the 1.6 mm LSP plates. a) and c) For the “Thick” plate case (10 mm thickness) and b) and d) for the actual thickness (1.6 mm) - ¼ axisymmetric expansion and magnification with a scale factor of 100

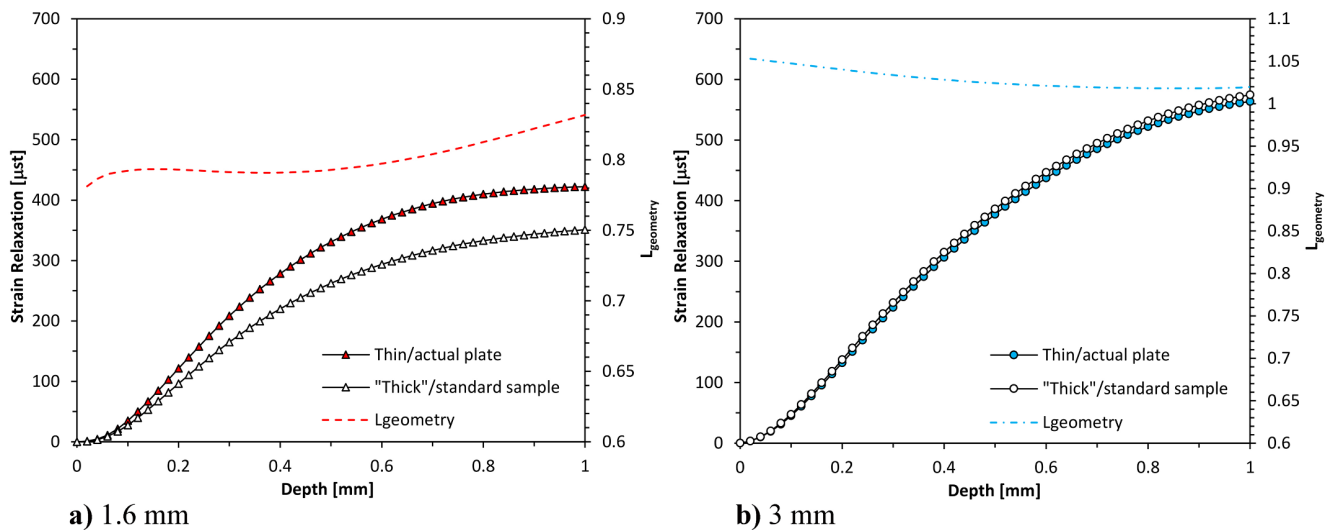


Fig. 10 FEM strain-depth relaxation curves for “thick” compared to “thin” samples and $L_{geometry}$ function for a) 1.6 mm and b) 3 mm thick plates, considering the simulated in-depth stress profiles shown in Fig. 8

between the strain relaxation curves shown are only due to the effect of the plate thickness. While for 3 mm plate thickness the effect is very small, it is significant for the case of 1.6 mm plate thickness. The ratio between both leads to the determination of $L_{geometry}(z)$ function, as per eq. (2), shown in the same figure (Fig. 9).

The averaged error through the whole hole depth, due to the thin thickness, is of 25% for the case of 1.6 mm plate thickness and lower than 5% for the case of 3 mm plate thickness. The correction function $L_{geometry}$ determined from both stress-depth relaxation curves, as per eq. (2), is also shown in Fig. 10. It is important to mention that FE analysis, using different stress distributions, such as a in depth uniform stress of 100 MPa and different materials, such as steel and aluminum, led to very similar correction functions $L_{geometry}$ and the obtained values are also very similar to those determined by Held et al. [16].

Considering the obtained correction function, $L_{geometry}$, the strain-depth relaxation curves experimentally obtained in the LSP samples were then corrected prior to use the integral method for residual stress calculation. Figure 11 shows the obtained results considering only the minimum principal stress component, for sake of clarity. As previously mentioned, the other stress components follow the same trend. In Fig. 11 the in-depth residual stress profiles determined by the integral method using the calibration coefficients (a and b) determined by FEM, considering the actual thickness of the plates, are also shown. It is clear that the results obtained using the $L_{geometry}$ function provide very similar results than those determined using the specific calibration coefficients determined by FEM (average error up to 3%). In addition, it is also clear that, for the case of the thinnest plates (1.6 mm), the new residual stress profiles determined by IHD, using the integral method and the experimentally obtained strain-depth

relaxation curves, using the specific FEM calibration coefficients, to consider the actual plate thickness, or the integral method using corrected strain-depth relaxation curves, based on the $L_{geometry}$ function, prior to use the ASTM standard, agree very well with the residual stress profiles obtained by XRD, ND and EDXRD techniques. Finally, considering the results obtained in plates with 3 mm thickness, the limit of 5.13 mm thickness recommended by ASTM seems to be conservative, despite that some thickness influence already exists. However, considering the observed dispersion of the results usually found during the residual stress evaluation by IHD, there is no absolute need to correct the results found in the 3 mm thickness plate, as shown in Fig. 11b. These results seem to confirm the thickness limit proposed by Sobolevski [17], since the corrected curves (solid lines) are within the uncertainty of IHD measurements.

Conclusions

Residual stresses in thin aluminum alloy 7075 plates, with different thicknesses and subjected to laser shock peening (LSP) treatment, were determined by the incremental hole drilling (IHD) technique and compared with those determined using diffraction techniques, used as reference. It was observed that the magnitude of residual stresses decrease when the thickness of the treated specimens decrease. LSP compressive residual stresses extend to a depth of more or less 1 mm, increasing with the increase of the plate thickness for the same LSP parameters, which is beneficial to avoid fatigue crack growth. The laser raster pattern strategy led to residual stresses slightly greater in the stepping direction than in the laser scanning direction and the differences increase when thickness decreases. While for thicker samples a good agreement

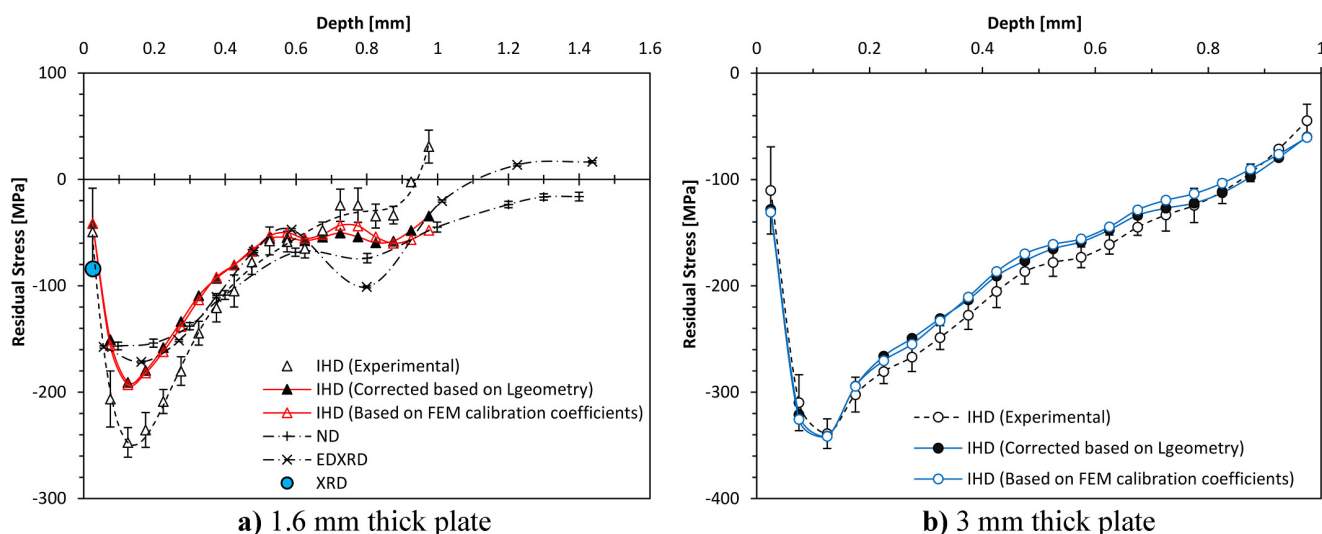


Fig. 11 Residual stresses determined experimentally in the LSP samples, with and without correction for the case of IHD measurement technique in **a)** 1.6 mm and **b)** 3 mm thick plates

between the results obtained by the different measurement techniques is observed, a clear discrepancy exists for the case of the thinnest plates (1.6 mm) analyzed. In this case, the residual stresses determined by IHD are overrated compared with those determined by diffraction. The use of an epoxy backing strategy to mitigate the influence of the thin thickness of the samples is clearly useless.

A finite element analysis (FEM) was carried out to understand the IHD in depth non uniform residual stress results, obtained in specimens with thicknesses of 1.6 mm and 3 mm, respectively, which are falling out the limits preconized by the ASTM E837 ($< D = 5.13$ mm). FEM simulated strain-depth relaxation curves present an averaged error of 25% for the case of 1.6 mm plate thickness, being lower than 5% for the case of 3 mm plate thickness, compared to the case of a “thick” plate evaluation. The use of a correction function, L_{geometry} , to correct the experimentally obtained strain-depth relaxation curves, enables to still use the ASTM standard procedure, with an averaged error up to 3% in respect to the evaluation using the integral method and specific calibration coefficients for its use in thin plates. From the practical point of view, the use of such correction function is reliable and can provide the wanted results, considering the dispersion usually found during the IHD tests, substantially decreasing the effort to accurately determine the in-depth non uniform residual stresses by IHD in thin plates, i.e., when the thickness is below the limits preconized by the ASTM standard.

Acknowledgments The authors would like to acknowledge the DSI-NRF Centre of Excellence in Strong Materials (CoE-SM) for their financial support. They would also like to acknowledge the vital support of the South African Centre for Scientific and Industrial Research National Laser Centre’s (CSIR NLC) Rental Pool Program (RPP), funded by the Department of Science and Innovation (DSI). In addition, this work is based on the research supported in part by the National Research Foundation (NRF) of South Africa through the Incentive Funding for Rated Researchers (IFRR), Equipment-Related Travel and Training Grant (ERTTG) (Grant Numbers: 109200 and 115195) and under the Competitive Programme for Rated Researchers (Grant Number: 106036). Opinions, findings and conclusions or recommendations expressed in this work are those of the authors and are not necessarily to be attributed to the CoE-SM or to the NRF. Finally a special acknowledgement to Dr. Daniel Glaser from CSIR for his precious assistance on LSP technology.

References

1. ASTM E837-13a (2013) Standard test method for determining residual stresses by the hole-drilling strain-gage method, ASTM International, West Conshohocken, PA, www.astm.org
2. Schajer GS, Whitehead PS (2018) Hole-drilling method for measuring residual stresses. Synthesis SEM Lectures on Experimental Mechanics 1(1):1–186. <https://doi.org/10.2200/S00818ED1V01Y201712SEM001>
3. Frija M, Hassine T, Fathallah R, Bouraoui C, Dogui A (2006) Finite element modelling of shot peening process: prediction of the compressive residual stresses, the plastic deformations and the surface integrity. Mater Sci Eng A 426(1):173–180. <https://doi.org/10.1016/j.msea.2006.03.097>
4. Hammond DW, Meguid SA (1990) Crack propagation in the presence of shot peening residual stresses. Eng Fract Mech 37(2):373–387. [https://doi.org/10.1016/0013-7944\(90\)90048-L](https://doi.org/10.1016/0013-7944(90)90048-L)
5. Furfari D (2014) Laser shock peening to repair, design and manufacture current and future aircraft structures by residual stress engineering. Adv Mater Res 891-892:992–1000. <https://doi.org/10.4028/www.scientific.net/AMR.891-892.992>
6. García-Granada AA, Gomez-Gras G, Jerez-Mesa R, Travieso-Rodríguez JA, Reyes G (2017) Ball-burnishing effect on deep residual stress on AISI 1038 and AA2017-T4. Mater Manuf Process 32(11):1279–1289. <https://doi.org/10.1080/10426914.2017.1317351>
7. Troiani E, Taddia S, Meneghin I, Molinari G (2014) Fatigue crack growth in laser shock peened thin metallic panels. Adv Mater Res 996:775–781. <https://doi.org/10.4028/www.scientific.net/AMR.996.775>
8. Ocaña JL, Correa C, García-Beltrán A, Porro JA, Díaz M, Ruiz-de-Lara L, Peral D (2015) Laser shock processing of thin Al2024-T351 plates for induction of through-thickness compressive residual stresses fields. J Mater Process Technol 223:8–15. <https://doi.org/10.1016/j.jmatprotec.2015.03.030>
9. Petan L, Ocaña JL, Grum J (2016) Effects of laser shock peening on the surface integrity of 18% Ni Maraging steel. Strojniški vestnik - Journal of Mechanical Engineering 62(5):291–298. <https://doi.org/10.5545/sv-jme.2015.3305>
10. Prime MB (2000) Cross-sectional mapping of residual stresses by measuring the surface contour after a cut. J Eng Mater Technol 123(2):162–168. <https://doi.org/10.1115/1.1345526>
11. Kartal ME (2013) Analytical solutions for determining residual stresses in two-dimensional domains using the contour method. Proceedings of the Royal Society a: mathematical, physical and engineering sciences 469(2159):20130367. <https://doi.org/10.1098/rspa.2013.0367>
12. Kartal ME, Liljedahl CDM, Gungor S, Edwards L, Fitzpatrick ME (2008) Determination of the profile of the complete residual stress tensor in a VPPA weld using the multi-axial contour method. Acta Mater 56(16):4417–4428. <https://doi.org/10.1016/j.actamat.2008.05.007>
13. Staden SNV, Polese C, Glaser D, Nobre JP, Venter AM, Marais D, Okasinski J, Park J-S (2018) Measurement of Residual Stresses in Different Thicknesses of Laser Shock Peened Aluminium Alloy Samples. Materials Research Proceedings 4:117–122. <https://doi.org/10.21741/9781945291678-18>
14. Toparli MB (2012) Analysis of residual stress fields in aerospace materials after laser peening. PhD Dissertation, The Open University, Milton Keynes, UK
15. Toparli MB, Fitzpatrick ME (2016) Development and application of the contour method to determine the residual stresses in thin laser-peened Aluminium alloy plates. Exp Mech 56(2):323–330. <https://doi.org/10.1007/s11340-015-0100-7>
16. Held E, Schuster S, Gibmeier J (2014) Incremental hole-drilling method Vs. thin components: a simple correction approach. Adv Mater Res 996:283–288. <https://doi.org/10.4028/www.scientific.net/AMR.996.283>
17. Sobolevski EG (2007) Residual stress analysis of components with real geometries using the incremental hole-drilling technique and a differential evaluation method. PhD dissert., Kassel University, Kassel, Germany
18. Gore B, Nobre JP (2016) Effects of numerical methods on residual stress evaluation by the incremental hole-drilling technique using the integral method. Materials research proceedings 2:587–592. <https://doi.org/10.21741/9781945291173-99>
19. Schajer GS (1988) Measurement of non-uniform residual stress using the hole-drilling method. Part II-practical application of the

- integral method. *Journal of Eng mat and tech (ASME)* 110(4):344–349. <https://doi.org/10.1115/1.3226060>
20. Magnier A, Zinn W, Niendorf T, Scholtes B (2019) Residual stress analysis on thin metal sheets using the incremental hole drilling method – fundamentals and validation. *Exp Tech* 43(1):65–79. <https://doi.org/10.1007/s40799-018-0266-x>
 21. Schuster S, Steinzig M, Gibmeier J (2017) Incremental hole Drilling for Residual Stress Analysis of thin walled components with regard to plasticity effects. *Exp Mech* 57(9):1457–1467. <https://doi.org/10.1007/s11340-017-0318-7>
 22. Nobre JP, Kornmeier M, Scholtes B (2018) Plasticity effects in the hole-drilling residual stress measurement in peened surfaces. *Exp Mech* 58(2):369–380. <https://doi.org/10.1007/s11340-017-0352-5>
 23. Schajer GS, Whitehead PS (2018) Hole-drilling method for measuring residual stresses, vol 1. Synthesis SEM Lectures on Experimental Mechanics, vol 1. Morgan & Claypool Publishers. doi: <https://doi.org/10.2200/S00818ED1V01Y201712SEM001>
 24. Lorentzen T (2003) Anisotropy of lattice strain response. In: Fitzpatrick M, Lodini A (eds) *Analysis of residual stress by diffraction using neutron and synchrotron radiation*. CRC Press, London
 25. *ASM Handbook* (1990), vol 2. Properties and Selection: Nonferrous Alloys and Special-Purpose Materials. ASM International
 26. Macherauch E, Müller P (1961) Das sin2 ψ -Verfahren der Röntgenographischen Spannungsmessung. *Zeitschrift für Angewandte Physik* 13:305–312
 27. ANSYS I (2013) *ANSYS Mechanical APDL Theory Reference*. Release 15.0 edn. SAS IP, Inc., Canonsburg, USA
 28. Schajer GS (1981) Application of finite element calculations to residual stress measurements. *Journal of Eng mat and tech (ASME)* 103(2):157–163. <https://doi.org/10.1115/1.3224988>
 29. Kornmeier M (1999) *Analyse von Abschreck- und Verformungseigenstressen mittels Bohrloch- und Röntgenverfahren*. PhD Dissertation, Universität Gh Kassel, Kassel, Germany
 30. Schajer GS (1993) Use of displacement data to calculate strain gauge response in non-uniform strain fields. *Strain* 29(1):9–13. <https://doi.org/10.1111/j.1475-1305.1993.tb00820.x>
 31. Correa C, Peral D, Porro JA, Díaz M, Ruiz de Lara L, García-Beltrán A, Ocaña JL (2015) Random-type scanning patterns in laser shock peening without absorbing coating in 2024-T351 Al alloy: a solution to reduce residual stress anisotropy. *Opt Laser Technol* 73: 179–187. <https://doi.org/10.1016/j.optlastec.2015.04.027>
 32. ANSYS I (2013) *ANSYS advanced analysis techniques*. SAS IP, Inc., Canonsburg

Publisher's Note Springer Nature remains neutral with regard to jurisdictional claims in published maps and institutional affiliations.

